Wire Initiation Critical for Radiation Symmetry in *Z*-Pinch–Driven Dynamic Hohlraums

T. W. L. Sanford,[1] C. A. Jennings,[1] G. A. Rochau,[1] S. E. Rosenthal,[1] G. S. Sarkisov,[2] P. V. Sasorov,[3] W. A. Stygar,[1] L. F. Bennett,[1] D. E. Bliss,[1] J. P. Chittenden,[4] M. E. Cuneo,[1] M. G. Haines,[4] R. J. Leeper,[1] R. C. Mock,[2] T. J. Nash,[1] and D. L. Peterson[5]

[1]*Sandia National Laboratories, Albuquerque, New Mexico 87185, USA*
[2]*Ktech Corporation, Albuquerque, New Mexico 87123, USA*
[3]*Institute of Theoretical and Experimental Physics, Moscow 117218, Russia*
[4]*Imperial College, London SW7 2BW, United Kingdom*
[5]*Los Alamos National Laboratory, Los Alamos, New Mexico 87545, USA*
(Received 2 August 2006; published 9 February 2007)

Axial symmetry in x-ray radiation of wire-array z pinches is important for the creation of dynamic hohlraums used to compress inertial-confinement-fusion capsules. We present the first evidence that this symmetry is directly correlated with the magnitude of the negative radial electric field along the wire surface. This field (in turn) is inferred to control the initial energy deposition into the wire cores, as well as any current shorting to the return conductor.

DOI: 10.1103/PhysRevLett.98.065003 PACS numbers: 52.58.Lq, 52.57.Fg, 52.59.Qy

Dynamic hohlraums (DH) driven by a z pinch [1] are being developed and used as intense blackbody x-ray sources for inertial confinement fusion [2,3] and high temperature (>200 eV) radiation-transport experiments [4]. They are among the most intense sources available in the laboratory for these applications. In our DH configurations [Fig. 1(a)], two nested coaxial cylindrical arrays of tungsten wires form a z-pinch plasma shell [5] that generates x rays as it impacts on a low-opacity cylindrical foam target, centered on the z-pinch axis, filling the target region with x rays. Central to the utility of the DH is the assumption that the radiation is axially symmetric about the target center. Because of the axial symmetry of the z pinch (aside from the power feed), radiation exiting from the top and bottom radiation exit holes [REHs, Fig. 1(a)] is expected to be identical [6]. However, in experiments, more peak x-ray (0.2–4 keV) power always radiates from the top REH relative to the bottom [6]. This observation is independent of whether the imploding array is nested or not [6].

Here we present new data that clearly show a strong correlation between the axial x-ray asymmetry and the structure of the negative radial electric field E_r between the surface of the wires in the outer array and the current-return can [grounded outer cylinder, Fig. 1(a)]. This field controls the axial energy deposition to the individual wires during the wire-initiation phase, when current [Fig. 1(b)] first flows through the outer array O approximately 70–90 ns prior to the start of the main power pulse, which has a rise time of ~100 ns. Hence, we establish for the first time a connection between wire initiation and x-ray production symmetry in wire-array z pinches.

The experiments were fielded on the 20-MA Z generator at Sandia National Laboratories using a DH configuration [Fig. 1(a)] similar to those discussed in Refs. [4,6]. Aside from being developed to understand the axial asymmetry, the experiments were designed to maximize the axial power as a function of outer-array diameter ($24 < \phi < 56$ mm) and outer-array wire number ($108 < N < 540$). Two coaxial nested arrays were used such that the inner array was half the diameter of the outer, the inner wire number was half that in the outer, and the mass of the inner was half the outer, with the mass of the central foam target equal to the sum of the inner and outer arrays. The 40 mm diameter outer array with 240 wires [4] maximized the axial x-ray power and is referred to as the baseline configuration. For all arrays except one, the implosion time was kept fixed by simultaneously adjusting the outer-array mass m and radius r such that $m\,r^2$ remained constant. The exception was a configuration in which the masses of the inner and outer arrays of the baseline were reversed [7] by reducing the outer wire diameter (from 7.4 to 5.2 μm) and increasing the inner wire diameter (from 7.4 to 10.5 μm). This change slightly reduced the implosion time. In all cases the separation of the outer wire array and the return conductor Δ was kept constant at 5 mm.

The 8-mm-high target used [T in Fig. 1(a)] was offset from either electrode by 3-mm-high hollow pedestals. The pedestals prevented tungsten-wire-array plasma generated near the electrodes from prematurely crossing the REHs, prior to the arrival of the main plasma shell [7]. The pedestal was particularly beneficial on the cathode side K, where significantly more early tungsten was observed to flow relative to the anode side A. The tungsten led to increased opacity at the REHs. The axially resolved x-ray streak camera image in Fig. 1(c) illustrates the need for the pedestal located at the cathode. The early streak image near −13 ns, below ~3 mm, corresponds to early tungsten being stopped by the pedestal. Zero defines the time of stagnation (maximum of radial x-ray power [4]). Prior to the use of the pedestals, the peak top-to-bottom power ratio of the baseline configuration was 2 ± 0.5 [6].

 © 2007 The American Physical Society

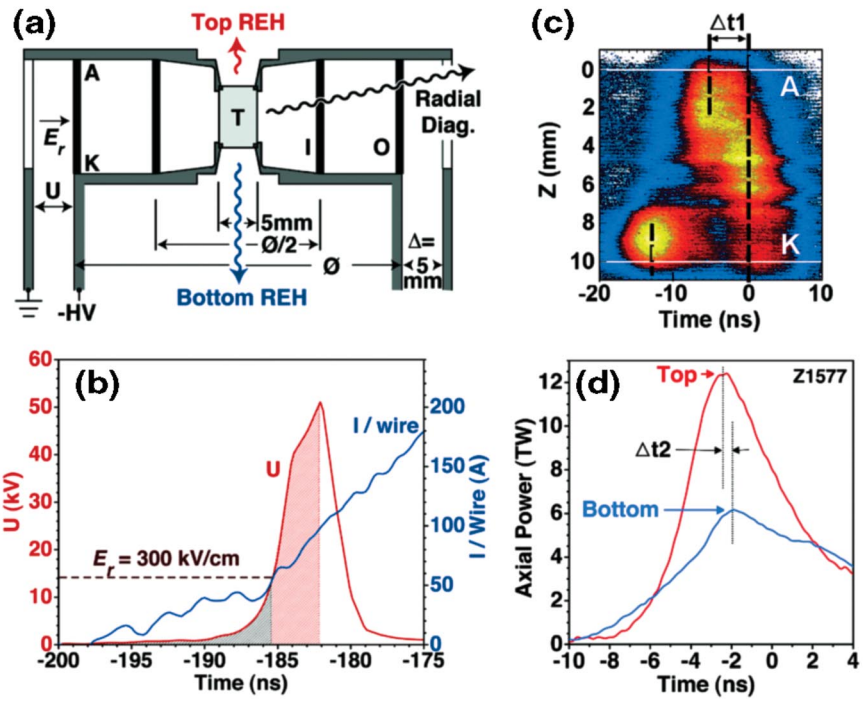

FIG. 1 (color). (a) Experimental arrangement, showing anode A, cathode K, target T, inner array I, outer array O, electric field E_r across AK gap Δ, and AK voltage U, (b) experimental current and resistive voltage drop U across the wires for baseline configuration, (c) axial x-ray streak camera image ($\Delta t1$-zipper time), and (d) associated top-bottom axial powers for baseline configuration (Z shot 1577), illustrating top-bottom peak-power time difference $\Delta t2$. In (b)–(d), zero time refers to time of stagnation.

With the pedestals, the top-to-bottom power ratio decreased to 1.1 ± 0.2. With the large, widely varying asymmetry mitigated by the pedestals, we have been able to observe the remaining radiation asymmetry [typical of Fig. 1(d)] more consistently as a function of one of the independent variables of our experiment, namely, E_r.

This field is negative in our experiments because of the location of the annular feed slot adjacent to the cathode [Fig. 1(a)]. Through this slot the Poynting vector $\boldsymbol{E} \times \boldsymbol{H}$ supplies electromagnetic energy for resistive dissipation in the wires, for magnetic (inductive) energy between the conducting wires and the return conductor, and for kinetic energy of the implosion. As a result, E_r essentially has a maximum amplitude at the cathode and falls nearly linearly to zero at the anode. Prior to plasma formation, if the number of wires N in the outer array of diameter Φ is large, so that $\ln(\Phi/N\Phi_w) \ll 2\Delta N/\Phi$, the minimum E_r occurs at the surface of each wire of diameter Φ_w and is given by [8]

$$E_r = Uz\Phi/\Delta l N \Phi_w, \tag{1}$$

assuming a constant gap Δ between the outer array and current return can and ignoring disturbances of the electric field by the diagnostic slots. U is the voltage at the feed, l is the length of the wire between the anode and cathode, and z is measured from the anode [Figs. 1(a) and 1(c)].

Even with a cathode pedestal, many shots [like Z1577 of Fig. 1(c)] show both large top-bottom power asymmetries [Fig. 1(d)] and "zippering" of the main plasma shell at stagnation, with the earliest arrival at the anode [Fig. 1(c)]. Zippering results in top REH emission peaking earlier and with a faster rise time than emission from the bottom [Fig. 1(d)] and thus provides an additional contribution to the axial asymmetry. Moreover, in our experiments with both top and bottom pedestals, for which the outer-array diameter Φ was systematically increased, the difference in the time of peak top-bottom axial powers [$\Delta t2$ in Fig. 1(d)] and the rise times grow nearly monotonically from small to large values, as illustrated in Fig. 2 for four sequential diameters. As the diameter increases, so does E_r at the

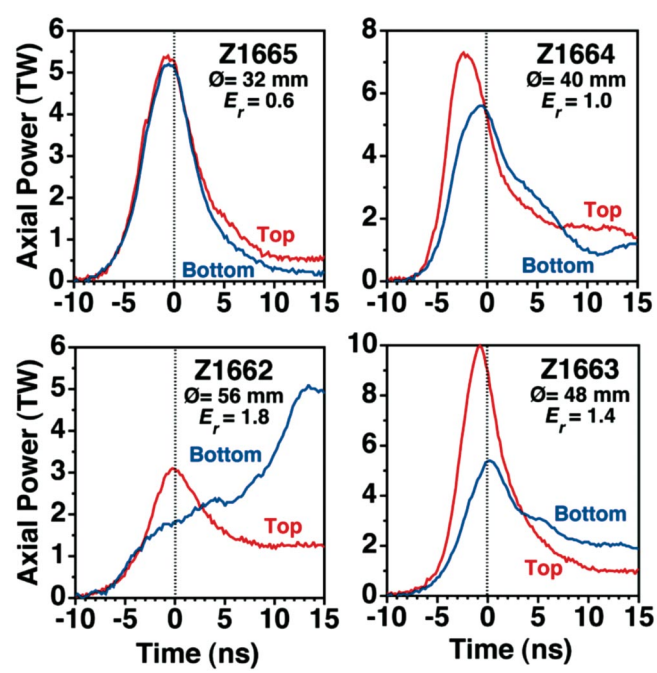

FIG. 2 (color). Top-bottom axial powers for four sequential Z shots with differing array diameters.

surface of the cathode end of the outer wires [Eq. (1)]. When all the data (including those where Φ_w and N were also varied) are plotted as a function of the relative E_r, the relative E_r appears to be a unifying predictor of the asymmetry, with higher E_r typically resulting in a larger range of asymmetry. Above a relative E_r of ~ 0.8, the axial powers [Fig. 3(a)], the times of the peak power [Fig. 3(b)], the rise times [Fig. 3(c)], and differences in the tungsten radiation fraction between top and bottom [Fig. 3(d)] begin to diverge significantly. Here, the relative E_r is defined as the radial electric field [Eq. (1)] at the midpoint ($l/2$) normalized by the field calculated for the baseline configuration, and is used as a dimensionless experimental parameter for correlating with the strength and timing of the axial asymmetry found in the x-ray emission. The tungsten fraction refers to the ratio of M-shell tungsten x rays measured between 2.0 and 2.4 keV relative to the total emission measured between 1.4 and 3.5 keV in time-integrating axial spectrometers [7].

This phenomenon may be understood as follows. E_r affects the current distribution at very early times when it can enhance electron emission from the wire cores and generate early breakdown of the vapor surrounding each wire. The current then shunts locally to this surrounding plasma of lower resistance, rather than stay in the core. In this way, as found in single-wire experiments [9], the wire cores will remain cold at the cathode end and will be hot at the anode end. Another possible effect at early times when the magnetic field is relatively weak is some temporary shorting of current to the return can near the cathode. This would be followed by axial sweeping through the $\boldsymbol{J} \times \boldsymbol{B}$ force of this current towards the anode, leading to an axial component of flow. For a given wire arrangement, therefore, the larger E_r becomes (always near zero at the anode end), the greater the energy-deposition imbalance between top and bottom becomes. The data in Fig. 3 thus suggest that axial radiation asymmetry scales with axial energy-deposition variation. To maintain symmetric deposition and associated radiation fields, the data also indicate that the relative E_r should remain below ~ 0.8.

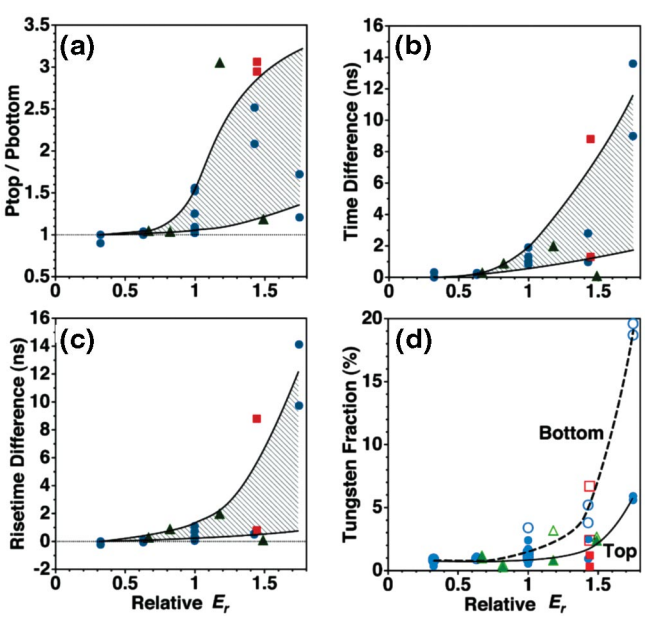

FIG. 3 (color). (a) Top-bottom power ratio at time of peak top axial power, (b) top-bottom peak-power time difference [$\Delta t2$ in Fig. 1(d)], (c) top-bottom rise-time difference, and (d) top and bottom tungsten radiation fractions vs relative E_r. Open data points in (d) correspond to bottom measurements. Circle, triangle, and square data correspond to array diameter, wire number, and mass reversal scans. The lines are only to help guide the eye.

As a first step in simulating the effect of the varying energy deposition and subsequent array implosion within the baseline configuration, we first estimate the energy deposited in a single baseline wire in the absence of E_r. The voltage [Fig. 1(b)] corresponding to an outer wire in the baseline configuration is calculated using the measured current [Fig. 1(b)] as input to a 1D resistive magnetohydrodynamic (RMHD) simulation with the MACH2 code [9]. In the simulation, when current flows in the wire it Joule heats and expands. This change reduces its conductivity, producing an increased resistive voltage drop along the wire, and results in the development of a low-density, very low-conductivity metallic vapor layer at the wire surface [9]. The voltage collapses when the outer metallic vapor layer Joule heats to ionization at -182 ns [Fig. 1(b)], producing a rapidly expanding hot metallic plasma. Single-wire experiments [9], however, show domination of a light impurity vapor contribution to breakdown for low-current rate explosions (as is the case here), which precedes the breakdown of metal vapor alone. The calculated voltage may thus peak higher and later than the actual voltage, and so provides only an upper limit of the energy deposited to the wire core.

Next, to estimate the difference in energy deposition between cathode and anode parts of the wire we assume that earlier cathode side breakdown occurs when E_r reaches the field emission threshold of [10] ~ 300 kV/cm [Fig. 1(b)]. In practice there is little need to distinguish between thermionic emission [11] (enhanced by the Schottky effect with negative E_r) and field emission, as they both occur near the same time, namely, at -185 ns [Fig. 1(b)]. The important point is that whatever the source of electrons (thermionic or field emission) the inward-directed z-dependent E_r enhances emission and accelerates the electrons into the surrounding vapor to trigger its ionization [9] before thermal ionization occurs. This leads to 2.8 eV/atom less specific energy deposited into the cathode end of the wires relative to the anode and hence a temperature difference of ~ 0.7 eV between the two ends.

Incorporating the above, we modified (in the full baseline configuration including wires) the initial temperature of the preexpanded gaseous wire cores in the RMHD code

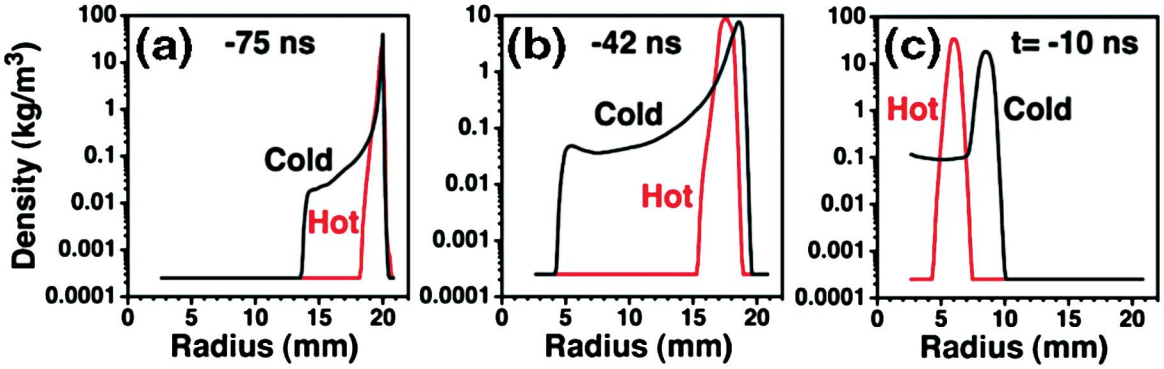

FIG. 4 (color). (a)–(c) Azimuthally averaged mass distributions following implosion of the 40-mm diameter baseline array for hot and cold initial core temperatures in GORGON.

GORGON [12] to reflect the estimated cathode-anode temperature difference. A 3D wedge geometry modeled a single wire in the array. Figures 4(a)–4(c) show the azimuthally averaged mass distribution, for the implosion of the 40-mm-diameter tungsten array, assuming two different initial core temperatures: a cold one (to reflect conditions near the cathode) and a hot one (to reflect conditions near the anode). For simplicity, the inner array is neglected. The array with the lower initial temperature persists as a cold core, ablating material for a prolonged period of time before running out of material and beginning to implode. As the implosion proceeds, precursor material contained within the array is snowplowed up, essentially tamping the acceleration of the imploding surface. This situation exemplifies what may occur near the cathode because of early current shunting. The precursor plasma partly represents what we see early in time on the cathode side being blocked, in part, by the bottom pedestal [Fig. 1(c)]. For the high initial temperature, which represents what may occur near the anode with little or no current shunting, the wire ablation proceeds more rapidly. The higher mass ablation rate results in a lower velocity of the ablated material and formation of little precursor plasma. Experimentally, little precursor plasma is seen at the anode. The core-corona structure does not persist for a prolonged period, and the implosion is more shell-like [5]. With earlier complete wire ablation, less material is present within the array to be snowplowed up and the array implodes more quickly, allowing the shell to reach the axis prior to the corresponding cold-core implosion. These two simulations represent extremes of conditions at either end of the wires. Between the ends, current shunting will gradually occur later as the anode is approached [9], resulting in a zippered stagnation as seen experimentally [Fig. 1(c)]. The simulated time difference of the zipper (4 ± 0.5 ns) is in agreement with the 4.3 ± 1.0 ns measured [$\Delta t1$ in Fig. 1(c)] for four shots like that of Z1577.

The general phenomena simulated and measured are likely related to observations at low wire numbers [13,14], where the implosion was found to depend only on the "polarity" of the radial electric field, and not its magnitude as here. In Ref. [14], the polarity effect [9] depends strongly on the initial-current rate of rise. Variation in this rate among the shots discussed here may account for the asymmetry variations when the relative E_r exceeds $\sim$0.8 (Fig. 3).

In summary, there is a marked correlation between the degree of axial asymmetry in radiation power and timing and the relative radial electric field E_r. To minimize the asymmetry it is necessary to keep the relative E_r below 0.8. The likely physical mechanisms are the preferential breakdown and ionization of the vapor surrounding each wire at the cathode end, together with the possibility of transient current shorting here to the return current can.

Sandia is a multiprogram laboratory operated by the Sandia Corporation, a Lockheed Martin Company, for the U.S. DOE under Contract No. DE-AC04-94AL85000.

[1] T. W. L. Sanford *et al.*, Plasma Phys. Controlled Fusion **46**, B423 (2004).
[2] T. W. L. Sanford *et al.*, Phys. Rev. Lett. **83**, 5511 (1999).
[3] C. L. Ruiz *et al.*, Phys. Rev. Lett. **93**, 015001 (2004).
[4] T. W. L. Sanford *et al.*, Phys. Plasmas **9**, 3573 (2002).
[5] T. W. L. Sanford *et al.*, Phys. Rev. Lett. **77**, 5063 (1996).
[6] T. W. L. Sanford *et al.*, Phys. Plasmas **10**, 1187 (2003).
[7] T. W. L. Sanford *et al.*, Phys. Plasmas **12**, 022701 (2005); **12**, 122701 (2005).
[8] G. S. Sarkisov *et al.*, Bull. Am. Phys. Soc. **46**, 28 (2001).
[9] G. S. Sarkisov *et al.*, Phys. Rev. E **71**, 046404 (2005); **66**, 046413 (2002).
[10] D. J. Johnson *et al.*, IEEE Trans. Dielectr. Electr. Insul. **13**, 52 (2006).
[11] W. B. Nottingham, Phys. Rev. **49**, 78 (1936).
[12] J. P. Chittenden *et al.*, Plasma Phys. Controlled Fusion **46**, B457 (2004).
[13] S. N. Bland *et al.*, Phys. Rev. Lett. **95**, 135001 (2005).
[14] G. M. Oleinik *et al.*, J. Phys. IV (France) **133**, 779 (2006).